ELSEVIER

Biophysical Chemistry 74 (1998) 71–82

Biophysical Chemistry

X-ray diffraction studies on the structural changes of rigor muscles induced by binding of phosphate analogs in the presence of MgADP

Duck-Sool Kim[1,a], Yasunori Takezawa[a], Masaki Ogino[a], Takakazu Kobayashi[b], Toshiaki Arata[c], Katsuzo Wakabayashi[a,*]

[a] *Division of Biophysical Engineering, Graduate School of Engineering Science, Osaka University, Toyonaka, Osaka 560-8531, Japan*
[b] *Department of Physiology, School of Medicine, Teikyo University, Itabashi-ku, Tokyo 173-0003, Japan*
[c] *Department of Biology, Graduate School of Science, Osaka University, Toyonaka, Osaka 560-0043, Japan*

Received 13 March 1998; received in revised form 30 April 1998; accepted 30 April 1998

Abstract

To clarify the structure of the ATP hydrolysis intermediates (ADP.P_i bound state) formed by actomyosin crossbridges, the effects of various phosphate analogs in the presence of MgADP on the structures of the thin and thick filaments in glycerinated rabbit *psoas* muscle fibers in the rigor state have been investigated by X-ray diffraction with a short exposure time using synchrotron radiation. When MgADP and phosphate analogs such as metallofluorides ($BeF_{x=3,4}$ and AlF_4) and vanadate ($VO_4(V_i)$) were added to rigor fibers in the presence of the ATP-depletion backup system, the intensities of the actin-based layer lines were markedly weakened. The greatest effect ($\sim 50\%$ decrease in intensity) was observed in the presence of BeF_x among the analogs examined. The intensity distribution of the 5.9 nm actin-based layer line shifted towards that observed in the Ca^{2+}-activated fibers, while the first actin layer line at $\sim 1/36.7\ nm^{-1}$ retained a rigor-like profile with an intensity weakened by $\sim 50\%$. The intensity of the equatorial 10 reflection increased while that of the 11 reflection changed little, resulting in only a small increase (~ 1.7 fold) in the intensity ratio of the 10 to the 11 reflection. No resting-like pattern appeared upon the addition of MgADP and BeF_x. These results indicate that a substantial fraction ($\sim 40\%$) of the myosin heads dissociate from actin but the detached heads remain in the vicinity of the actin filaments when MgADP and BeF_x

* Corresponding author. Tel./fax: +81 6 8506515; e-mail: waka@bpe.es.osaka-u.ac.jp
[1] Present address: Department of Chemical Technology, College of Engineering, Chang-Won National University, Chang-Won, Kyung Nam 641-773, Korea.

0301-4622/98/$19.00
PII S0301-4622(98)00166-5

bind. The states produced by binding phosphate analogs to a rigor muscle differ from the resting-like state produced by adding them to a contracting muscle (Takemori et al., J. Biochem. (Tokyo) 117 (1995) 603–608). Our conclusion put forward to explain the data is that one of the two heads of a crossbridge is detached and the other retains a rigor-like attachment.

Keywords: Effect of ADP binding; Effects of ADP and phosphate analogs; Conformation of myosin heads; X-ray diffraction; Synchrotron radiation

1. Introduction

There is as yet little direct evidence concerning the configurations of attached crossbridges in the intermediate states which are supposed to exist during the cyclical hydrolysis of ATP by actomyosin in muscle. It is important to investigate the relationship between elementary biochemical states and structural states of the actomyosin crossbridge cycle in a skeletal muscle. To this end, the effects of binding of various ATP analogs and phosphate analogs on muscle crossbridge structure have been extensively studied by a number of investigators (reviewed by Cooke [1]). It is well known that ADP and vanadate ($VO_4(V_i)$) bind to the myosin heads forming a myosin-ADP-V_i ternary complex and is a good analog for the myosin-ADP-phosphate (M.ADP.P_i), a predominant steady state intermediate of the ATP hydrolysis cycle [2–4]. More recently, it has also been found that metallofluorides such as aluminum fluoride (AlF_4) and beryllium fluoride ($BeF_{x=3,4}$) may act as a phosphate analog [5,6] and form ternary complexes with myosin (myosin-ADP-AlF_4 (M.ADP.AlF_4) and myosin-ADP-BeF_x (M.ADP.BeF_x)) in the presence of Mg ions and ADP [7,8]. The structures of these ternary complexes as well as an ADP complex have been examined with *Dictyostelium* truncated myosin by X-ray crystallography [9–11] and with a chicken skeletal myosin subfragment-1 (S1) by X-ray solution scattering [12,13], suggesting that binding of these phosphate analogs is stabilizing specific crossbridge configurations.

These phosphate analogs have been known to bind to actively cycling heads in a contracting muscle and inhibit active tension almost completely [3,14–16]. However, one of these analogs, vanadate, did not bind or bound weakly to attached heads in a rigor muscle and dropped tension only slightly [3]. In contrast, X-ray diffraction patterns from an insect flight muscle in rigor changed towards resting patterns when it was incubated for 12–24 h with vanadate and MgADP [17]. Solution studies have shown that vanadate binds to an actomyosin–ADP complex, which is formed by adding ADP to actomyosin, and dissociates it, although the protein concentration under these conditions is much lower than in muscle [2,8]. Therefore, it is not clear whether these phosphate analogs can bind to the heads when they are attached stereospecifically to actin filaments in a rigor muscle, and whether phosphate analogs can stabilize a crossbridge configuration in a different intermediate attached state.

We report here that MgADP and these phosphate analogs can bind to the attached heads in the rigor state and cause significant structural changes as detected by X-ray diffraction. The present X-ray results suggest that when ADP and BeF_x bind to actin, roughly 40% of the heads are dissociated from actin, but they still remain in the vicinity of the thin filaments or are interacting weakly with actin. The structural nature of these attached heads bearing an ADP.BeF_x as an ADP.P_i analog in the rigor state will be discussed by comparing these data with that obtained in a contracting state and in the light of the two-headed structure of a myosin molecule. A preliminary result was reported in the abstract form [18].

2. Materials and methods

2.1. Specimen preparation

Rabbit *psoas* muscles were glycerinated by

conventional methods (e.g. Tawada and Kimura [19]). Muscle fibers were used within 2 weeks after glycerination. The specimens for X-ray diffraction experiments consisted of bundles ~0.2 mm in diameter and 6 mm in length containing 10–15 single fibers, which were isolated in glycerin-containing solution. The sarcomere length of the fiber bundle was adjusted to ~2.4 μm using optical diffraction with a He–Ne laser. Such bundles were mounted in a Perspex chamber with two Mylar windows to pass X-rays through. After washing out the glycerination solution, rigor solution (80 mM K-propionate, 5 mM EGTA, 6 mM Mg-acetate and 40 mM imidazole/HCl buffer (pH 7.0)) was circulated through the chamber. To prevent the build-up of ATP and decompose contaminating ATP in the solution, inhibitors for muscle adenylate kinase (0.2 mM diadenosine pentaphosphate (AP_5A)) and 0.1 mg or ~3 units/ml hexokinase — 1 mM glucose system (the ATP-depletion backup system) were added to the rigor solution containing 1 mM MgADP. For the experiments with MgADP and vanadate (V_i), a stock solution of vanadate, which was prepared according to Goodno and Taylor [2], was added to the ADP solution to a final concentration of 1–1.5 mM. For those with ADP and metallofluorides, 5 mM NaF and 1 mM $BeSO_4$ or $AlCl_3$ were added to the ADP solution according to Maruta et al. [7]. Relaxing solution consisted of rigor solution plus 5 mM Na_2ATP. Activating solution consisted of relaxing solution plus 2 mM $CaCl_2$.

2.2. X-ray diffraction experiments

X-ray experiments were performed at the Beamline 15A at the Photon Factory (Tsukuba, Japan), using synchrotron radiation from a positron storage ring. Monochromatic X-ray beam (wavelength, $\lambda = 0.1507$ nm) was selected and collimated by using double focusing optics [20]. The storage ring was operated at 2.5 GeV with a beam current between 300 and 350 mA. The fiber bundle was set horizontally so as to make the optimum use of collimated X-ray beams. The size of the X-ray beam was 2.3 (H) $\times$ 0.4 (V) mm at the specimen.

X-ray diffraction patterns were recorded on a storage phosphor area detector (Fuji image plate (type BAS-III), Fuji Film, Tokyo) (see, Amemiya et al. [21]) with a specimen-to-plate distance of 130 cm. Exposure time was typically 30–45 s to record up to the 2.7 nm meridional actin reflection. Three diffraction patterns were recorded from the same specimen sequentially; the first record was taken from the specimen in rigor solution containing MgADP, the second one from the specimen in solution containing MgADP and a phosphate analog and the last one from the specimen again in rigor solution containing MgADP to observe the extent of recovery of the original pattern. Patterns were recorded from the specimens in relaxing solution to confirm that the muscles can still go into the fully relaxed state. Patterns from muscle in the active state were also recorded during the plateau of tension from the specimen after passing activating solution through the chamber. No appreciable indication of radiation damages of the specimen was observed after a total exposure of less than 3 min. During exposure to X-rays, the experimental solution was continuously circulated through the specimen chamber with a peristaltic pump. The temperature was maintained at 20°C to avoid any effect of low temperatures on the X-ray pattern from this muscle at relaxed state [22–24]. Before each X-ray exposure, the specimen was incubated in the desired solution for at least 30 min (except for activating solution). After the exposure, the image plate was scanned by an image reader (BAS 2000, Fuji Film, Tokyo) using a pixel size of 100×100 μm. To minimize the variation in the intensity measurements, the same image plate was used for each series of experiments.

2.3. Intensity measurements and data analysis

X-ray data from the image plates were analyzed on graphic workstations (PC-98RL, NEC, Tokyo), Sparc Station 330 (Sun Microsystems, USA) and Power Macintosh 7200 (Apple Computer Inc., USA). After determining the origin of the images and correcting the inclination angle of each image, the four quadrants of the patterns were folded and averaged, and data from three

muscles were usually added to increase the signal-to-noise ratio. The intensities between the original patterns and those with analogs were scaled by the total intensity in the whole area of the diffraction pattern (excluding the area around the beam stop and the strong equatorial region) [25]. The intensity distributions of the layer lines were measured by scanning the data perpendicular to the layer lines (parallel to the meridian) at intervals of two pixels. The background line under each peak was drawn by connecting linearly minimum points on each side of the peak. The integrated intensity was obtained by summing up the digital data in the area above the background line and plotted as a function of the reciprocal radial coordinate, R ($=2\sin\Theta/\lambda$ where Θ is half the scattering angle and λ, the X-ray wavelength used) to obtain a layer-line profile. In addition, in order to directly obtain the integrated intensity of the whole layer-line reflections as well as the meridional reflections, the axial intensity distribution of the reflection was measured by radial integration, on stripes parallel to the meridian with radial ranges appropriate to the layer-line reflections. For each axial intensity of the reflection, a line was drawn by connecting two background points on each side of the peak, and the integrated intensity was obtained by summing up the data in the area above the line.

3. Results

3.1. Intensity changes of the actin-based layer lines by addition of MgADP and phosphate analogs

Fig. 1 shows a pair of X-ray diffraction patterns from rabbit muscle fibers in ADP-rigor (left half) and in the presence of MgADP and BeF_x (right half) as a typical example showing the effects of binding MgADP and phosphate analogs. The X-ray patterns observed in the presence of MgADP and a phosphate analog retained the basic features of the rigor pattern, but the intensities of most of the actin-based layer lines were weakened. The intensity profiles of these layer lines also tended to be slightly broader in the axial direction. There was no major changes in the axial spacing of the layer lines and meridional reflections. The weakening of the layer lines was accompanied by an increase in the background intensity as depicted in a difference pattern (Fig. 2) which was made between those as shown in Fig. 1. The intensity changes of various actin-based layer lines (the first one at a reciprocal axial spacing at $\sim 1/36.7$ nm^{-1}, the fifth at $\sim 1/7.2$ nm^{-1}, the sixth at $\sim 1/5.9$ nm^{-1}, seventh at $\sim 1/5.1$ nm^{-1} and the meridional reflection at $\sim 1/2.7$ nm^{-1}) are depicted in Fig. 3 which shows the results of MgADP and BeF_x binding. The effects of the other analogs are similar but occur to a lesser extent than this, possibly due to their slow time course of binding. The relative effectiveness of the various analogs in producing structural changes as judged from the intensity reduction appeared to be in the order of BeF_x, V_i and AlF_4 when examined at a fixed time (~ 30 min) after starting incubation as depicted in Fig. 4, corresponding to the order of the strength in their reactivity in solution [7]. In all three analogs, layer-line intensities changed in an analogous manner. A gradual drop of the rigor tension was also observed in the same order (data not shown), indicating trapping of ADP.P_i analogs on the myosin heads. Although binding of these phosphate analogs was slow, in the case of BeF_x the rigor tension fell to a 20% level at ~ 30 min after starting incubation and the X-ray pattern did not change appreciably with further incubation of 1 or 2 h, showing that the structural change was mostly completed after 30 min. The results in the following sections refer to those obtained from the muscle with ADP and BeF_x unless otherwise stated.

In Fig. 3, it is noted that the first (36.7 nm), fifth (7.2 nm) and seventh (5.1 nm) actin-based layer lines decreased in integrated intensity while retaining their lateral profile along the layer line. There was also a substantial decrease in the intensity of the second layer line (18.6 nm) (see Fig. 1). On the other hand, the intensity of the sixth (5.9 nm) layer line decreased by $\sim 30\%$ with a marked reduction in the meridional side of the intensity distribution, resulting in an intensity profile more similar to that observed in the resting state (Fig. 5). When compared with that in the Ca^{2+}-activated state, it was found that the lateral

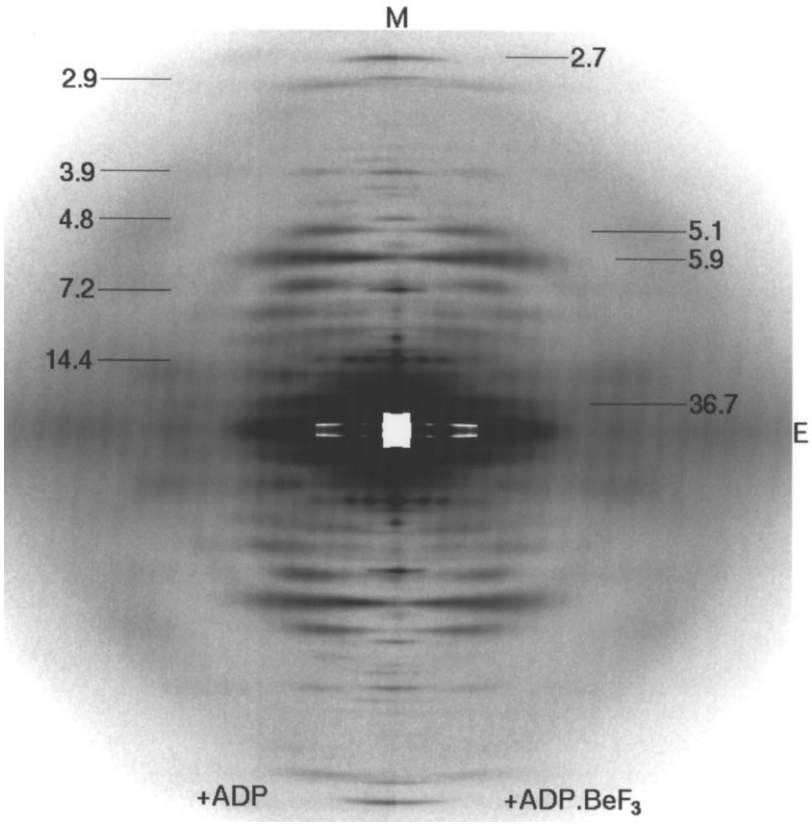

Fig. 1. Comparison of X-ray diffraction patterns in the presence of MgADP (left half) and the presence of MgADP and BeF_x (right half). Each half pattern is shown with the meridional axis (vertical) aligned with the other. The experiments were performed as described in Section 2, and 1 mM MgADP and 1 mM BeF_x were added to the rigor solution. The solution contained the ATP-depletion backup system APsA to avoid ATP contamination and generation. X-ray patterns were exposed for 30 s. The appropriate Gaussian form background intensity was subtracted for illustration purpose. The fiber axis is vertical; M, the meridional axis and E, the equatorial axis. Representative layer-line reflections are denoted by the approximate axial spacing. Note that overall patterns are very similar but most of the actin-based reflections became weaker in the presence of BeF_x.

profile of the 5.9 nm layer line resembled rather closely that of the Ca^{2+}-activated state (Fig. 5). The intensity of the 2.7 nm meridional actin reflection decreased (by $\sim 45\%$), the decrease in the meridional region being much greater than in the outer region.

Fig. 6 summarizes the changes in the integrated intensities of these actin-based reflections from the muscle bound with ADP and BeF_x. When the values from the rigor muscle with ADP are taken as a reference (cf. ADP binding causes small intensity changes [26,27]), the amount of intensity decrease was $\sim 53\%$ for the first layer line, $\sim 52\%$ for the 8.9 nm layer line, $\sim 58\%$ for the 7.2 nm layer line, $\sim 30\%$ for the 5.9 nm layer line, $\sim 22\%$ for the 5.1 nm layer line and $\sim 45\%$ for the 2.7 nm meridional reflection. Among these reflections, the intensities of the 8.9 nm, 7.2 nm and 2.7 nm reflections were too weak to measure in the resting state, and the resting intensity of the first layer line is estimated to be less than 15% of the rigor intensity. On the other hand, the resting intensities of the 5.9 nm and 5.1 nm layer-line reflections were about 40% and 35% of their rigor intensities, respectively. Thus, the intensity of these layer lines is reduced to a value (0.5 ± 0.15) approximately midway between the rigor and resting intensities by binding of ADP

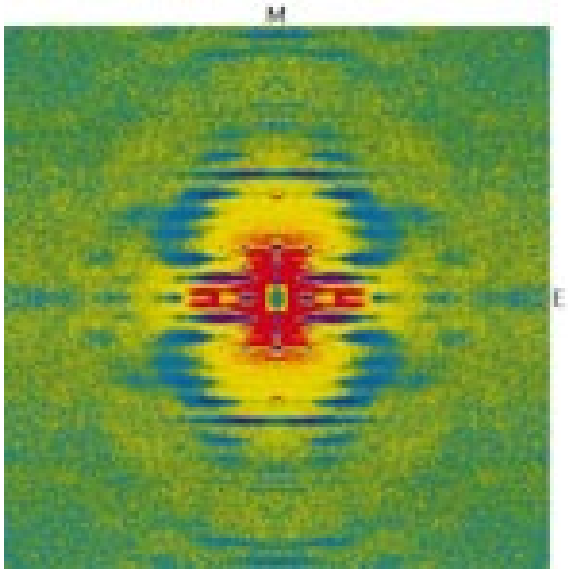

Fig. 2. A difference pattern made by subtracting the digital data of the rigor-MgADP pattern from the rigor-MgADP.BeF_x pattern recorded from the same muscles as shown in Fig. 1. The green (0 level) through yellow to red colors indicate increasing intensities, the blue to violet decreasing intensities. The orientation of the pattern is the same as in Fig. 1. Note that the intensities of the diffuse scattering in the small-angle region are intensified in the presence of MgADP and BeF_x due to an increase in substitution disorder and disordered arrangement of detached heads.

and BeF_x. As does the lateral shift in the 5.9 nm layer line, such a large intensity reduction implies dissociation of a fairly large number of the myosin heads from the actin filaments rather than conformational changes of the heads which remain attached. However, upon addition of MgADP and phosphate analogs to a rigor muscle, no resting-like myosin layer lines appeared, suggesting that any dissociated myosin heads which seem to have bound ADP.P_i analogs do not assume the ordering of the resting state as they appeared to when added to muscle in the contracting state [15].

3.2. Intensity changes of the equatorial reflections and the meridional reflections with a 14.4-nm-repeat by addition of MgADP and phosphate analogs

Fig. 7 shows the intensity changes of the equatorial 10 and 11 reflections upon addition of MgADP and BeF_x. The intensity of the 10 reflection increased markedly (by $\sim 50\%$) while that of the 11 reflection decreased slightly (by $\sim 10\%$). The intensity ratio of the 10 to the 11 reflections increased from 0.23 to 0.40 towards that in the relaxed state (0.83). This change (0.17) corresponds to $\sim 30\%$ of the rigor-to-resting change ($0.83 - 0.23 = 0.6$). The relatively small change in the 10/11 intensity ratio would also indicate that most of the detached heads are still in the vicinity of the thin filaments.

Fig. 8 shows the intensity changes of the first and second meridional reflections with a 14.4-nm-repeat. The intensity of the first reflection at $1/14.4\ nm^{-1}$ decreased by about 20% while retaining the subsidiary peaks, whereas that of the second order reflection at $1/7.2\ nm^{-1}$ increased by $\sim 44\%$. The clear presence of subsidiary peaks on the 14.4 nm meridional layer line (see also Fig. 1) indicates that the binding of ADP.P_i analogs does not affect the lattice structure in the rigor state. Those of the other higher order reflections of this repeat showed little change. There were no appreciable spacing changes of these reflections. The binding of ADP.BeF_x caused a reciprocal change in the intensities of the first and second 14.4-nm-based meridional reflections. Fig. 9 summarizes the intensity changes of these two meridional reflections together with the two inner equatorial reflections. Note that the meridional layer-line reflection at $\sim 1/3.9\ nm^{-1}$ mostly unchanged upon binding ADP.P_i analogs, suggesting that the backbone structure of the thick filaments was not affected by the addition of ADP.P_i analogs [26,27]. Similar intensity changes of the equatorial and 14.4-nm-based reflections were observed in binding of the other analogs.

4. Discussion

We aimed to look for any evidence of a new or specific configuration of the attached crossbridges in the intermediate states which is supposed to occur in the active process. The effects of ADP and phosphate analogs on the rigor state of crossbridges were studied in expectation that the analog-bound state might be, biochemically, equivalent to a short-lived state before the final state of

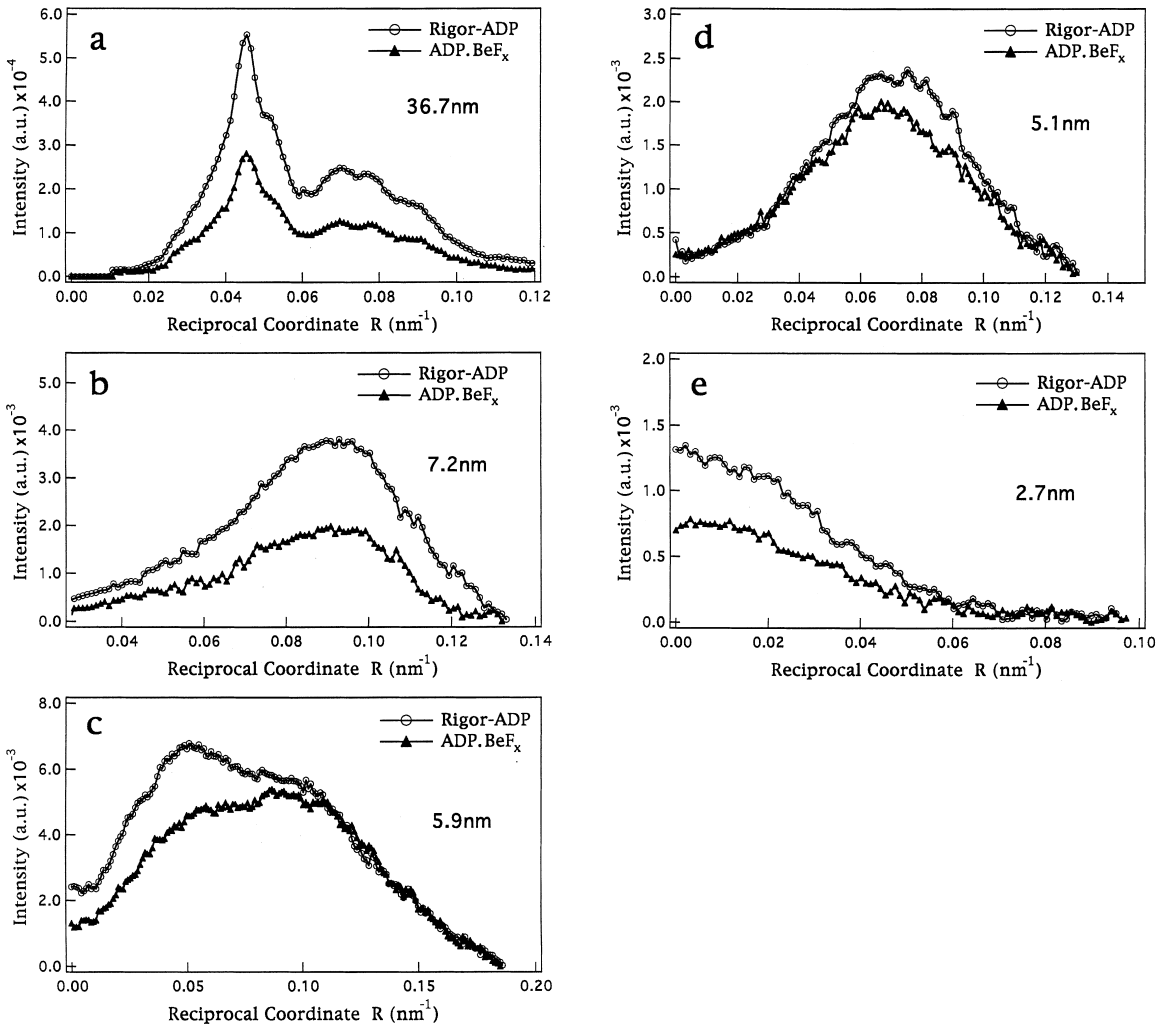

Fig. 3. Changes in the intensity profiles of actin-based layer lines from a rigor muscle in the presence of 1 mM MgADP and 1 mM phosphate analog (BeF_x). (a) The first actin layer line at a reciprocal axial spacing at $\sim 1/36.7\ nm^{-1}$, (b) the fifth at $\sim 1/7.2\ nm^{-1}$, (c) the sixth at $\sim 1/5.9\ nm^{-1}$, the seventh at $\sim 1/5.1\ nm^{-1}$ and (e) the meridional reflection at $\sim 1/2.7\ nm^{-1}$. In (a)–(e): ○, rigor-MgADP (control); ▲, +MgADP + BeF_x.

the ATP hydrolysis cycle. A structural comparison between the analog-bound state and the rigor or rigor-ADP bound states may provide information on structural changes in the actomyosin interaction. In the present study, we have shown that addition of phosphate analogs to a rigor muscle in the presence of MgADP results in a structural state clearly different from the rigor-ADP bound state [27].

Although we did not attempt to obtain biochemical evidence for formation of M.ADP.P_i-analogs in the present study, the X-ray diffraction pattern changed markedly and the rigor tension dropped upon addition of P_i-analogs to a rigor-ADP muscle. The intensity changes were largely reversible when MgADP and phosphate analogs were washed out, though full recovery occurred with a very slow time course. The X-ray pattern did not change further after prolonged incubation (> 30 min) in the case of ADP and BeF_x (1–1.5 mM). A

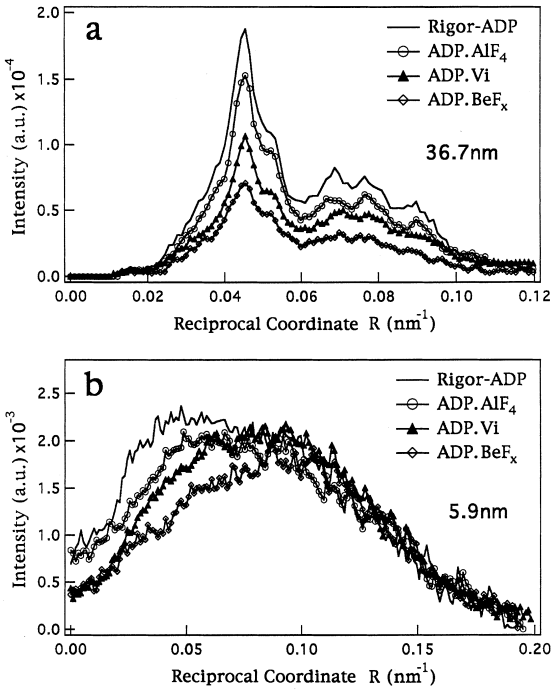

Fig. 4. Comparison of changes in the intensity profiles of the actin-based layer lines when various phosphate analogs (1 mM) were added to a rigor muscle with MgADP. (a) The first layer line at $\sim 1/36.7$ nm^{-1}, (b) the seventh layer line at $\sim 1/5.9$ nm^{-1}. In (a) and (b): —, rigor-MgADP (control); ○, +MgADP + AlF_4; ▲, +MgADP + V_i; ◇, +MgADP + BeF_x. These data were taken from diffraction patterns at a fixed time after starting incubating each solution containing MgADP and phosphate analog.

twofold increase in the concentration of phosphate analogs did not affect the results. These observations suggest that in our experiments the effects of addition of phosphate analogs (BeF_x) are saturated. After the experiments with analogs, the muscles were tested for relaxation with ATP, and they fully relaxed.

First, the intensity of the 10 equatorial reflection shows an increase of about 50% while the 11 reflection does not show a concomitant reduction. This indicates that the mass is not removed from the vicinity of the thin filaments when MgADP and phosphate analogs bind to crossbridges in a rigor muscle. These intensity changes resemble those occurring in relaxed muscles when ionic strength is lowered, where a large population of the resting myosin heads are thought to be attached weakly to the actin filaments [28,29]. The change in the intensity ratio (I_{10}/I_{11}) is about

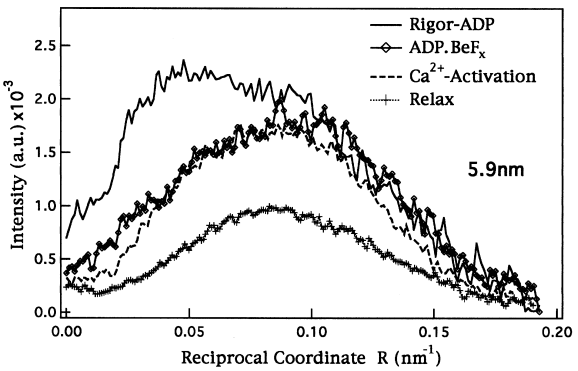

Fig. 5. Comparison of the intensity profile of the 5.9 nm actin layer line in the presence of MgADP + BeF_x and those in the other states of muscle. —, rigor-MgADP state; ◇, in the presence of MgADP + BeF_x; – – –, Ca^{2+}-activated state; +, relaxed state. Note that the profiles are very similar between MgADP + BeF_x and Ca^{2+}-activated (contracting) states.

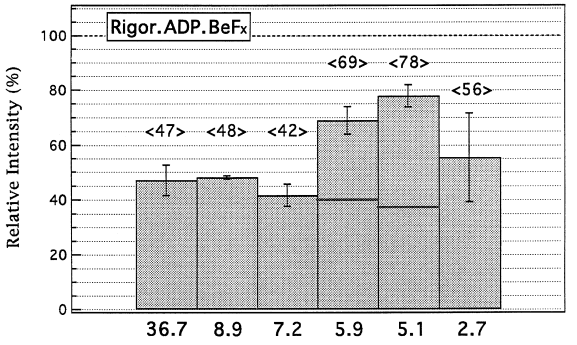

Fig. 6. Integrated intensities of the various actin-based layer-line reflections after addition of MgADP and BeF_x to a rigor muscle. The value of each reflection in the rigor-MgADP state is normalized as 100. The numbers on the abscissa denote the layer lines with a respective axial spacing. The integrated intensities were measured by radial integration in the ranges of $0.021 \le R \le 0.120$ nm^{-1} for the 36.7 nm layer line, $0.069 \le R \le 0.158$ nm^{-1} for the 8.9 nm layer line, $0.04 \le R \le 0.135$ nm^{-1} for the 7.2 nm layer line, $0 \le R \le 0.185$ nm^{-1} for the 5.9 nm layer line, $0 \le R \le 0.120$ nm^{-1} for the 5.1 nm layer line and $0 \le R \le 0.055$ nm^{-1} for the 2.7 nm meridional reflection. Each bar in the graph represents the mean and associated S.D. of three observations. Near each bar the average value is given in braces. Note that for the 5.9 nm and 5.1 nm reflections, their relative values in the relaxed state are shown in the bar graphs and those in the other layer lines are negligibly small in the relaxed state (see text).

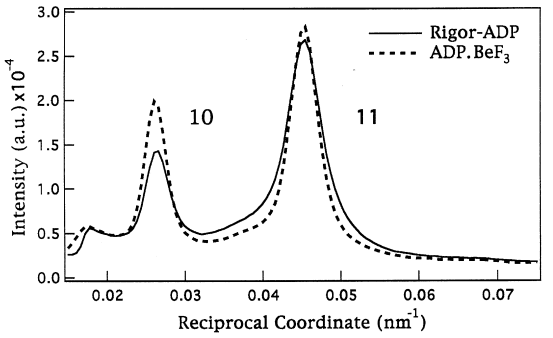

Fig. 7. Equatorial intensity profiles from the rigor muscle in the presence of MgADP (solid line) and of MgADP and BeF_x (chain line). The 10 and 11 reflections are seen at $R = 0.026$ nm^{-1} and 0.045 nm^{-1}, respectively.

30% of the rigor-to-resting change upon binding of MgADP and BeF_x (Fig. 9), suggesting that if any, a small fraction of heads ($< 30\%$) are fully detached or that most of the detached heads are still in the vicinity of the thin filaments.

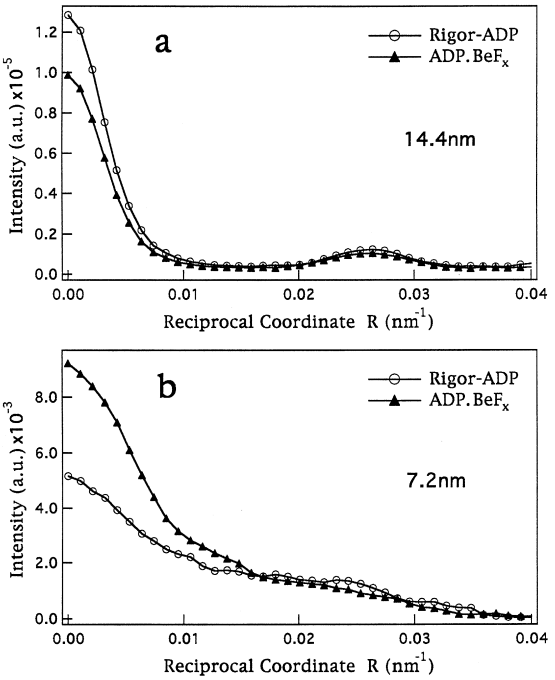

Fig. 8. Intensity profiles of the first and second meridional reflections with a 14.4-nm-repeat from the rigor muscle in the presence of MgADP (○) and the presence of MgADP and BeF_x (▲). (a) The first reflection at $1/14.4$ nm^{-1}, and (b) the second one at $1/7.2$ nm^{-1}.

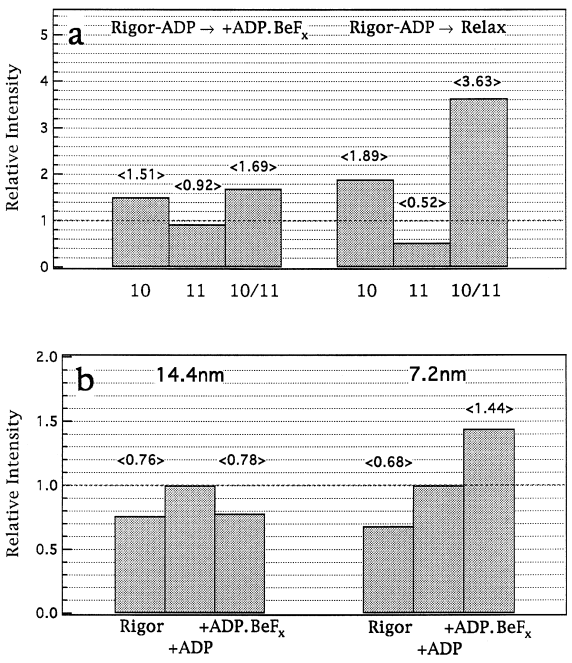

Fig. 9. Integrated intensities of the 10 and 11 equatorial reflections (a) and the 14.4 nm and 7.2 nm meridional reflections (b) by addition of BeF_x to a rigor muscle with MgADP. In (a) and (b), the value of each reflection from a muscle with MgADP is normalized as unity. In (a), 10/11 denotes the intensity ratio of the 10 and 11 reflections. The ratio in the rigor-ADP state was ~ 0.23. The integrated intensities of the 10 and 11 reflections were obtained in the range of $0.021 \leq R \leq 0.032$ nm^{-1} and $0.032 \leq R \leq 0.058$ nm^{-1}, respectively, and those of the 14.4 nm and 7.2 nm meridional reflections were measured in the range of $0 \leq R \leq 0.140$ nm^{-1} and $0 \leq R \leq 0.033$ nm^{-1}, respectively.

The same conclusion can be reached by intensity changes in the actin-based layer lines. A marked intensity decrease in all of the actin layer lines occurs upon binding of ADP and phosphate analogs to the attached heads. It has recently been reported that phosphate analogs such as metallofluorides bind to actin in the thin filament, causing instability of the filament structure at relatively high concentration [30]. Because the concentration of phosphate analogs is low in our X-ray experiments, and this actin-binding proceeds with a much slower time course than that of the present intensity changes, the observed intensity decrease in the actin-based layer lines is not due to an inducement of such instability. As

does the shift of the 5.9 nm actin layer line towards the high radius (Fig. 5), the changes we find in the actin layer lines could reflect that a significant number of myosin crossbridges have detached from actin filaments upon binding phosphate analogs. However, X-ray patterns show no signs of the characteristic relaxed myosin layer lines. Although a resting myosin layer-line pattern in a rabbit muscle is known to be weakened when the temperature is lowered [22–24], the lack of appearance of any resting-like features in the diffraction pattern is not due to such a temperature effect on this muscle, because the present experiments are performed at 20°C. The overall X-ray layer-line pattern retains rigor-like features.

In order to assess a population of detached heads from actin, we assume that the intensities of the rigor layer lines from the thin filaments are approximately determined by the occupancy of attached heads [31,32] as $I \propto (F_A + qF_M)^2$, where F_A and F_M denote the form factors of the actin monomer and myosin head, respectively, and q is the occupancy of the myosin heads on the actin lattice. This formula is derived on the assumption that the distribution of heads along the actin filament is random. We also assume that their intensities in the resting and rigor states correspond to 0 and 100% attachment ($q \sim 0.6$) of the myosin heads to actin filaments, respectively. Using simple spherical models for an actin and a myosin head with different radii and weights, the intensity changes of several layer lines were calculated as a function of occupancy. Then a population of the dissociated heads was estimated to be roughly 40% from the intensity reduction ($\sim 50\%$ on average) of the actin-based layer lines when ADP and BeF_x bound (see Fig. 6). The absence of the resting-like myosin layer lines such as the first myosin component at $\sim 1/43$ nm^{-1} indicates that the detached heads do not form a helix around the shaft of the thick filament as in the resting state but reside in the vicinity of the actin filaments. An increased background intensity (see Fig. 2) implies that these heads appear disordered or attach weakly/non-stereospecifically to actin. This increase in the background intensity can be also produced by an increase in substitution disorder [32] due to the detachment of heads. The present X-ray results would appear to contradict the previous X-ray diffraction studies [15] which reported that M.ADP.V_i formed in active muscle fibers leaves the vicinity of the actin filaments and generates a resting myosin helix. Thus, this lack of the myosin resting pattern in the present experimental data may be of some significance.

According to a simple probabilistic calculation based on the assumption of $\sim 40\%$ dissociation of the attached heads induced by binding of ADP and phosphate analogs, there are three species of the crossbridges: detached or weakly-attached crossbridges ($\sim 20\%$); single-headed binding (one rigor-like and the other weakly-attached) crossbridges ($\sim 50\%$); rigor-like double-headed binding crossbridges ($\sim 30\%$). Here we assume that there is no cooperativity between heads upon binding to actin filaments. The presence of $\sim 80\%$ of the total heads near the actin filaments may be consistent with the small change in the equatorial intensity ratio, because all of the crossbridges which are attached to actin regardless of strong or weak association would contribute to the equatorial pattern. However, the presence of $\sim 20\%$ fully dissociated crossbridges would be expected to give rise to myosin layer lines if they assume a resting configuration, which was not observed here. Because in the experiments with ADP.V_i by Takemori et al. [15], about 20–30% full dissociation produced strong appearance of the first myosin layer-line component. Alternatively, when we assume cooperativity between heads upon binding to the actin filaments, we can predict many kinds of distribution among above three crossbridge states (detached, single- and double-headed binding) based on $\sim 40\%$ dissociation of heads. In a most extreme case, when phosphate analogs bind, one of the two rigor heads of each myosin crossbridge detaches in the vicinity of actin filaments while the other head still retains its rigor attachment. Here we assume a strong negative cooperativity between two heads of each crossbridge upon binding to the actin filaments. This model may be more plausible than the first one, because there is no full dissociation of the crossbridges which is consistent with the lack of the myosin layer-line component.

Electron microscopic (EM) studies [33–36] and electron paramagnetic resonance (EPR) studies on spin-label orientation [37] have revealed that one of two heads in a rigor myosin crossbridge might be strained, and it is possible that such a strained head dissociates more easily than the other in the presence of nucleotide. In this connection, a notable difference in the diffraction pattern from a muscle with ADP and BeF_x as compared with rigor or rigor-ADP bound muscles is that the 5.9 nm layer line closely resembles that of Ca^{2+}-activated muscle (Fig. 5). (Note that the inner profile of this layer line is likely to be determined by the stereospecific two-headed binding of a myosin molecule.) Most recently, EM studies [38–40] and an EPR study [41] have revealed that during Ca^{2+}-activation the majority of crossbridges involve a single-headed binding with variable orientations to the actin filaments. The fact that the overall X-ray pattern retains rigor-like features is probably due to there being a strong, stereospecific rigor-like attachment of the other heads with a fixed orientation in accordance with the actin symmetry. In summary, our explanation put forward above suggests that there is one population of attached state (single-headed rigor-like binding crossbridges) in the presence of ADP and phosphate analogs but neither a mixture of resting-like and rigor-like crossbridges nor a probabilistic mixture of both types of heads. The conformational state produced by adding ADP and phosphate analogs to the rigor state may be one of the strongly-bound states which are supposed to exist during an active cycle.

Lastly, there are a decrease and an increase in the intensity of the first and second meridional reflections with a 14.4-nm-repeat, respectively (Fig. 8). Although the relatively strong appearance of the meridional reflections with this repeat in the rigor state (see Fig. 1) is not convincingly understood, the observed intensity changes could be taken as reflecting a conformational change of the attached heads because the axial positions of crossbridges should be influenced by the axial repeat in the thick filament [42]. When the rigor crossbridges bind MgADP alone, the intensity of the 14.4 nm reflection increases by $\sim 20\%$ and that of the 7.2 nm reflection increases by $\sim 40\%$ (see Fig. 9b). Thus the intensity of the 7.2 nm reflection is enhanced markedly ($\sim$ 2-fold) while that of the 14.4 nm reflection returns to a rigor level by addition of ADP and BeF_x to a rigor muscle (Fig. 9b). These changes are very similar to those occurring when Mg-adenylylimidodiphosphate (Mg-AMPPNP) binds to the attached heads in a rabbit rigor muscle. These structural changes are probably due to changes in the attached rigor-like head close to an S2 part, partly causing the decrease in the near-meridional intensity and a lateral shift in the profile of the 5.9 nm layer line [43]. The same explanation may be applied to the present cases; the changes occurring upon binding of MgADP alone to a rigor crossbridge [25,26] could be amplified by binding phosphate analogs.

Acknowledgements

The authors wish to thank Drs Y. Sugimoto and Y. Amemiya for their kind help throughout experiments at the Photon Factory. Thanks are also due to Drs T.C. Irving and K. Namba for critical reading of the manuscript and their valuable comments and discussion. This work was supported in part by grants from the Ministry of Education, Science, Culture and Sports of Japan (No. 09480175 to KW) and the Grant-in-Aid for Scientific Research on Priority Areas (No. 09279103 to KW and No. 09279223 to TA) and from Yamada Science Foundation.

References

[1] R. Cooke, CRC Crit. Rev. Biochem. 21 (1986) 53–118.
[2] C.C. Goodno, E.W. Taylor, Proc. Natl. Acad. Sci. USA 79 (1982) 21–25.
[3] J.A. Dantzig, Y.E. Goldman, J. Gen. Physiol. 86 (1985) 305–327.
[4] T. Kawamura, K. Tawada, J. Biochem. (Tokyo) 91 (1982) 1293–1298.
[5] J. Bigay, P. Deterre, C. Pfister, M. Chabre, EMBO J. 6 (1987) 2907–2913.
[6] G.D. Henry, S. Maruta, B.D. Sykes, M. Ikebe, Biochemistry 32 (1993) 10451–10456.
[7] S. Maruta, G.D. Henry, B.D. Sykes, M. Ikebe, J. Biol. Chem. 268 (1993) 7093–7100.
[8] B.C. Phan, L.D. Faller, E. Reisler, Biochemistry 32 (1993) 7712–7719.

[9] A.J. Fisher, C.A. Smith, J. Thoden, et al., Biochemistry 34 (1995) 8960–8972.
[10] C.A. Smith, I. Rayment, Biochemistry 35 (1996) 5404–5417.
[11] A.M. Gulick, C.B. Bauer, J.B. Thoden, I. Rayment, Biochemistry 36 (1997) 11619–11628.
[12] Y. Sugimoto, M. Tokunaga, Y. Takezawa, M. Ikebe, K. Wakabayashi, Biophys. J. 68 (1995) 29s–34s.
[13] Y. Sugimoto, M. Tokunaga, K. Wakabayashi, J. Muscle Res. Cell Motility, 17 (1996) 286a, and to be submitted for publication.
[14] P.B. Chase, D.A. Martyn, M.J. Kushmerick, A.M. Gordon, J. Physiol. 460 (1993) 231–246.
[15] S. Takemori, M. Yamaguchi, N. Yagi, J. Biochem. (Tokyo) 117 (1995) 603–608.
[16] G.J. Wilson, S.E. Shull, R. Cooke, Biophys. J. 68 (1995) 216–226.
[17] R.S. Goody, W. Hofmann, M.K. Reedy, A. Magid, C. Goodno, J. Muscle Res. Cell Motility 1 (1980) 198–199a.
[18] D.-S. Kim, Y. Takezawa, Y. Sugimoto, T. Kobayashi, T. Arata, K. Wakabayashi, J. Muscle Res. Cell Motility 17 (1996) 286a.
[19] K. Tawada, M. Kimura, Biophys. J. 45 (1984) 593–602.
[20] Y. Amemiya, K. Wakabayashi, T. Hamanaka, T. Wakabayashi, H. Hashizume, T. Matsushita, Nucl. Instrum. Methods 208 (1983) 471–477.
[21] Y. Amemiya, K. Wakabayashi, H. Tanaka, Y. Ueno, J. Miyahara, Science 237 (1987) 164–168.
[22] J. Wray, J. Muscle Res. Cell Motility 8 (1987) 62a.
[23] T. Wakabayashi, T. Akiba, K. Hirose, et al., Adv. Exp. Med. Biol. 226 (1988) 39–48.
[24] J. Lowy, D. Popp, A.A. Stewart, Biophys. J. 60 (1991) 812–824.
[25] K. Wakabayashi, Y. Sugimoto, H. Tanaka, Y. Ueno, Y. Takezawa, Y. Amemiya, Biophys. J. 67 (1994) 2422–2435.
[26] S. Takemori, M. Yamaguchi, N. Yagi, J. Muscle Res. Cell Motility 16 (1995) 571–577.
[27] Y. Takezawa, D.-S. Kim, M. Ogino, Y. Sugimoto, T. Kobayashi, T. Arata, K. Wakabayashi, Biophys. J. (1998), in press.
[28] T. Matsuda, R.J. Podolsky, Proc. Natl. Acad. Sci. USA 81 (1984) 2364–2368.
[29] B. Brenner, L.C. Yu, R.J. Podolsky, Biophys. J. 46 (1984) 299–306.
[30] C. Combeau, M.-F. Carlier, J. Biol. Chem. 33 (1988) 17429–17436.
[31] J. Squire, The Structural Basis of Muscular Contraction, Plenum Press, New York, 1981, Chap. 10.
[32] J.M. Cowley, Diffraction Physics, North Holland, Amsterdam, 1975, Chap. 7.
[33] R. Craig, A.G. Szent-Gyorgyi, L. Beese, P. Flicker, P. Vibert, C. Cohen, J. Mol. Biol. 140 (1980) 35–55.
[34] E. Katayama, Jpn. J. Physiol. 45 (1995) S91–S92.
[35] H. Schmitz, M.C. Reedy, M.K. Reedy, R.T. Tregear, H. Winkler, K.A. Taylor, J. Mol. Biol. 264 (1996) 279–301.
[36] H. Schmitz, M.C. Reedy, M.K. Reedy, R.T. Tregear, K.A. Taylor, J. Cell Biol. 139 (1997) 695–707.
[37] T. Arata, J. Mol. Biol. 214 (1990) 471–478.
[38] L.L. Frado, R. Craig, J. Mol. Biol. 223 (1992) 5864–5871.
[39] K. Hirose, C. Franzini-Armstrong, Y.E. Goldman, J.M. Murray, J. Cell Biol. 127 (1994) 763–778.
[40] E. Katayama, J. Biochem. (Tokyo) 106 (1989) 751–770.
[41] C.L. Berger, D.D. Thomas, Biochemistry 32 (1993) 3812–3821.
[42] J.M. Squire, J.J. Harford, J. Muscle Res. Cell Motility 9 (1988) 340–358.
[43] R. Padron, H.E. Huxley, J. Muscle Res. Cell Motility 5 (1984) 613–655.